JOURNAL OF VIROLOGY, Oct. 1996, p. 6973–6981 Vol. 70, No. 10
0022-538X/96/$04.00+0

The Rotavirus Nonstructural Glycoprotein NSP4 Possesses Membrane Destabilization Activity

PENG TIAN,† JUDITH M. BALL, CARL Q. Y. ZENG, AND MARY K. ESTES*
Division of Molecular Virology, Baylor College of Medicine, Houston, Texas 77030

Received 2 January 1996/Accepted 26 June 1996

During a unique morphogenetic process, rotaviruses obtain a transient membrane envelope when newly synthesized subviral particles bud into the endoplasmic reticulum (ER). As rotavirus particles mature, they lose their transient membrane and a layer of the glycoprotein VP7 forms the virion outer capsid shell. The nonstructural glycoprotein NSP4 functions as an intracellular receptor in the ER membrane (K. S. Au, W. K. Chan, J. W. Burns, and M. K. Estes, J. Virol. 63:4553–4562, 1989), and it has been hypothesized that NSP4 is involved in the removal of the envelope during viral morphogenesis (M. K. Estes and J. Cohen, Microbiol. Rev. 53:410–449, 1989; B. L. Petrie, M. K. Estes, and D. Y. Graham, J. Virol. 46:270–274, 1983). The purpose of the present study was to determine if NSP4 has a direct membrane destabilization activity (MDA) by using liposome leakage assays and electron microscopic visualization of liposome, microsome, and viral envelope disruption. The fluorescent marker (calcein) incorporated into liposomes was released when the liposomes were incubated with purified NSP4. A region corresponding to amino acid residues 114 to 135 of NSP4 also released calcein from liposomes. $NSP4_{114–135}$ peptide-specific antibody completely blocked the MDA of the purified NSP4 protein. These results suggest that this region contains at least part of the functional domain of NSP4. Liposomes composed of phosphatidylcholine and microsomes (to simulate ER membranes) were broken when observed by electron microscopy after incubation with NSP4 or the $NSP4_{114–135}$ peptide. In contrast, the envelope of Sendai virus, which is derived from cytoplasmic membranes, and erythrocytes were not disrupted by NSP4 and the $NSP4_{114–135}$ peptide. These results provide direct evidence that NSP4 possesses MDA and suggest that it can cause ER membrane damage. Therefore, NSP4 might play an important role in the removal of the transient envelope from budding particles during viral morphogenesis. A model for the MDA of NSP4 in viral morphogenesis is proposed.

Rotaviruses are recognized as the most important cause of severe viral gastroenteritis in humans and animals. Rotaviruses are nonenveloped, triple-layered particles with a genome of 11 segments of double-stranded RNA. Rotaviruses have a unique morphogenesis in which particles obtain a transient membrane envelope that is formed by the budding of newly made subviral particles into the endoplasmic reticulum (ER) (11, 26). As rotavirus particles mature, they lose their transient membrane, and a layer of glycoprotein VP7 forms the virion outer capsid shell. The viral nonstructural glycoprotein NSP4 (NS28) functions as an intracellular receptor in the ER membrane and binds newly made subviral particles and probably also the spike protein VP4 (2, 3, 19). Transiently enveloped particles accumulate when glycosylation is blocked with tunicamycin (26), indicating that glycosylation is important for removal of the envelope. Glycosylation of VP7 is not required for viral maturation, because a nonglycosylated VP7 variant of SA11 rotavirus (clone 28) undergoes normal viral morphogenesis (26). Therefore, NSP4 has been proposed to be the protein involved in the removal of the envelope during viral morphogenesis (13, 26).

Our previous work indicates that expression of NSP4 results in increased intracellular calcium levels ($[Ca^{2+}]_i$) in insect *Spodoptera frugiperda* (Sf9) cells expressing endogenous NSP4 (37) and that the increased calcium levels are mobilized from the ER (36). A phospholipase C (PLC)-mediated pathway is activated when NSP4 or $NSP4_{114–135}$ synthetic peptide is added to cells exogenously. However, a PLC inhibitor does not affect the increased $[Ca^{2+}]_i$ in Sf9 cells expressing NSP4 endogenously. In addition, the basal calcium permeability of the ER in insect cells endogenously expressing NSP4 was evaluated by measuring the release of calcium induced by ionomycin, a calcium ionophore, or thapsigargin, an inhibitor of the ER Ca^{2+}-ATPase pump (35). Results from these previous studies suggest that there is a second pathway, distinct from PLC-inositol-1,4,5-triphosphate, causing changes in the ER permeability in cells expressing NSP4. We hypothesized that the expression of NSP4 in the ER membrane might directly change the ER membrane permeability. This paper reports studies that directly tested the effects of NSP4 on liposomes composed of phosphatidylcholine (PC) and microsomes (ER) and on the envelope of Sendai virus (representing plasma membranes) and human erythrocytes (plasma membranes) and localized at least part of the functional domain of NSP4 responsible for the observed membrane destabilization activity (MDA).

MATERIALS AND METHODS

Purification of NSP4 (NS28) and VP6. NSP4 was purified from 5×10^8 Sf9 cells infected at a multiplicity of infection of 2.0 PFU per cell with recombinant baculovirus pAC461-G10 expressing rotavirus gene 10. At 72 h postinfection, the cells were harvested, washed with phosphate-buffered saline (PBS), and lysed with 10 ml of lysis buffer (10 mM Tris-HCl [pH 8.1], 0.1 mM EDTA, 2% deoxycholate). The NSP4 lysate was diluted in 50 ml of equilibration buffer (20 mM Tris HCl [pH 8.1]), clarified by centrifugation for 30 min at 8,000 × *g*, and filtered through a 0.22-μm-pore-size filter (Costar, Van Nuys, Calif.). NSP4 was purified by fast protein liquid chromatography (FPLC) with a quaternary methylamine (QMA) anion-exchange column (Waters Chromatography Division, Milford, Mass.) preequilibrated with equilibration buffer. Fractions corresponding to 0.7 M NaCl with an NaCl linear gradient (0 to 1.6 M NaCl) were collected

* Corresponding author. Mailing address: Division of Molecular Virology, Baylor College of Medicine, One Baylor Plaza, Houston, TX 77030. Phone: (713) 798-3585. Fax: (713) 798-3586. Electronic mail address: mestes@bcm.tmc.edu

† Present address: Howard Hughes Medical Institute and Department of Cell Biology, Baylor College of Medicine, Houston, TX 77030.

and examined for NSP4 by an immunodot blot method. NSP4-rich fractions were pooled, dialyzed against equilibration buffer, filtered through a 0.22-μm filter, and further purified with the QMA column. The final purified NSP4 was dialyzed exhaustively against 50 mM NH_4HCO_3, and aliquots were lyophilized.

The purity of NSP4 was examined by sodium dodecyl sulfate-polyacrylamide gel electrophoresis (SDS-PAGE) followed by silver staining with a kit (Sigma, St. Louis, Mo.), densitometry scanning, and Western blot (immunoblot) analysis with an antipeptide antiserum against $NSP4_{114–135}$ (5). Following these analyses, the purity was estimated to be at least 70%. The total protein concentration was determined with a protein assay system (Bio-Rad Laboratories, Hercules, Calif.) with the NSP4 concentration estimated at 70% of the total concentration. In some experiments, NSP4 was further purified by immunoaffinity chromatography to confirm the results obtained with the semipurified protein. The immunoaffinity column contained immobilized purified immunoglobulin G (IgG) specific for the $NSP4_{114–135}$ peptide. The bound NSP4 was eluted from the column with 0.1 M Tris-HCl buffer (pH 2.8). This protein was at least 90% pure and had a similar profile to that shown in Fig. 1B when analyzed by Western blotting (data not shown).

A rotavirus structural protein, VP6, was used as a control in this study. VP6 was produced from recombinant baculovirus-infected Sf9 cells as described previously (39). Briefly, Sf9 cells were infected with pAc461/SA11-6 and harvested 6 days postinfection. The medium containing VP6 was clarified by centrifugation. Oligomeric VP6 in the clarified supernatant was pelleted through a sucrose cushion and subjected to banding in a CsCl gradient (39). SDS-PAGE and silver staining showed that the purified VP6 protein was >95% pure.

Synthetic peptides. All peptides were synthesized by F-moc (fluorenylmethoxycarbonyl) chemistry (9) at the Peptide Synthesis Facility, University of Pittsburgh, Pittsburgh, Pa., and purified by high-pressure liquid chromatography and gel filtration as described previously (5). These included rotavirus $NSP4_{114–135}$ (DKLTTREIEQVELLKRIYDKLT); mNSP4 131K (DKLTTREIEQVELLKRI KDKLT); $NSP4_{2–22}$ (EKLTDLNYTLSVITLMNNTLH); $NSP4_{90–123}$ (TTKDEI EQMDRVVKEMRRQLEMIDKLTTREIEQ); a Norwalk virus-specific peptide, NVSP (SHVAKIRGTSNGTVINLTELD); and a C-terminal Norwalk virus capsid peptide, NVCP (DTGRNLGEFKAYPDGFLTCV). An amphipathic pH-sensitive membrane-active peptide, JTS-1 (GLFEALLELLESLWELLLEA) (15), was kindly provided by Stephen Gottschalk, Department of Cell Biology, Baylor College of Medicine, and Louis Smith, Department of Medicine, Baylor College of Medicine.

Preparation of liposomes. PC in chloroform was obtained from Avanti Polar Lipids, Inc., Birmingham, La., and the fluorescent dye calcein (molecular weight, 622.5) was obtained from Sigma. Liposomes of PC containing 100 mM calcein (adjusted to pH 7.3 by the addition of 10 N sodium hydroxide) were prepared by a sonication method (7, 24). Briefly, the lipid-chloroform solution (containing 20 mg of PC in 2 ml) was dried under N_2. The dried lipid then was suspended in 2 ml of 100 mM calcein in 10 mM Tris-HCl (pH 7.3) by mild vortexing followed by sonication with a needle probe for 15 to 20 min (Sonifier cell disrupter 350; Branson Sonic Power Co., Danbury, Conn.). The sonicate, which contained mainly small, unilamellar vesicles, was applied to a column of Sephadex G-25 (Pharmacia) and eluted with 10 mM Tris-HCl (pH 7.3)–140 mM NaCl buffer. Fractions of 0.25 ml were collected. A 1-μl portion of each fraction was added to 2 ml of 150 mM sodium citrate buffer (pH 7.4), and the fluorescence change was measured before and after the addition of 5 μl of 20% Triton X-100 (Sigma) at 520 nm (excitation at 470 nm) with a 650-15 fluorescence spectrophotometer (Perkin-Elmer Corp., Norwalk, Conn.). Fractions with a fluorescence change ratio (the fluorescence after the Triton X-100 treatment compared with the fluorescence before the Triton X-100 treatment) greater than 20 were pooled and used in the liposome leakage assays and in electron microscopy studies.

Liposome leakage assays. Leakage of liposomal content in the presence of NSP4 or synthetic peptides was measured by the release of entrapped calcein (7). Calcein fluorescence was measured at 520 nm with a Perkin-Elmer fluorescence spectrophotometer. A 2-μl portion of liposome solution was added to 2 ml of 150 mM sodium citrate buffer (pH 5.0 to 7.4) or 140 mM NaCl–10 mM Tris-HCl buffer (pH 7.2). In some experiments, 100 nM to 10 mM calcium was added to the NaCl-Tris buffer. Various concentrations of purified NSP4 or synthetic peptides were incubated with the liposomes for 10 to 15 min. The value corresponding to 100% leakage was determined by measurement of the fluorescence released by complete lysis of liposomes after addition of 5 μl of 20% Triton X-100.

Preparation of $NSP4_{114–135}$ peptide-specific antibody and antibody blocking assay. $NSP4_{114–135}$ peptide-specific antiserum was generated in New Zealand White rabbits by multiple immunizations with 100 nmol of peptide cross-linked via glutaraldehyde to the protein carrier keyhole limpet hemocyanin as previously described (4). Pre- and postimmunization sera were evaluated by peptide enzyme-linked immunosorbent assay (4). IgG from the sera of rabbits was prepared by a simple two-step procedure described by McKinney and Parkinson (18). Briefly, albumin and other non-IgG proteins were precipitated with caprylic acid. Then the IgG fraction was precipitated with ammonium sulfate. For antibody protection assays, NSP4 protein was incubated with 10 μl of purified IgG for 30 min at 37°C before the mixture was incubated with liposomes.

EM. Liposomes and microsomes incubated with or without NSP4 protein/peptide or the other control peptides were examined by EM. Copper grids, coated with collodion-carbon and freshly glow discharged, were used for sample adsorption (40). Ammonium molybdate (1%; pH 6.5) was used as the negative stain. NSP4 (6 to 12 μM) protein in PBS or synthetic peptides (40 to 200 μM) in PBS were incubated with liposomes, microsomes (Promega), or purified enveloped Sendai virus for 15 min at room temperature. A grid was floated on a drop of sample for 20 min, excess fluid was removed by blotting with filter paper, and the dried grid was washed for 2 s on a drop of water, floated on 1 drop of stain for 15 s, and air dried. All electron micrographs were taken with a Philips CM 10 electron microscope operating at 80 kV.

Measurement of intracellular calcium level changes induced by NSP4 and synthetic peptides. $[Ca^{2+}]_i$ was measured by using the fluorescent Ca^{2+} indicator fura-2 as previously described (37). Briefly, 10^8 Sf9 insect cells were incubated for 30 min at room temperature in 20 ml of extracellular buffer (10 mM $CaCl_2$, 60 mM KCl, 17 mM $MgCl_2$, 10 mM NaCl, 10 mM morpholineethanesulfonic acid [MES], 4 mM glucose, 110 mM sucrose, 0.1% bovine serum albumin [pH 6.2]) containing 2 μM fura-2 acetoxymethyl ester fura-2/AM; Molecular Probes, Eugene, Oreg.). After being washed with extracellular buffer, aliquots of cells (5×10^6 cells) were placed in a quartz cuvette with a magnetic stirrer and fluorescence was measured before and after the addition of the synthetic peptides in a SLM 8000 spectrofluorimeter (SLM Instruments, Urbana, Ill.) with the excitation wavelength being altered between 340 and 380 nm and the emission fluorescence being recorded at 510 nm. All measurements were performed at room temperature and corrected for autofluorescence with unloaded cells. The fura-2 associated with the cells was calibrated by lysing the cells in the presence of saturated divalent cation followed by the addition of ethylene glycol-bis(β-aminoethyl ether)-*N*,*N*,*N*′,*N*′-tetraacetic acid (EGTA; pH 8.5). $[Ca^{2+}]_i$ was calculated from the equations of Grynkiewicz et al. (16) with an equilibrium dissociation constant (K_d) for Ca^{2+} binding to fura-2 of 278 nM at 22°C (34).

Hemolysis assays. Hemolysis assays were performed as described by Gottschalk et al. (15). Briefly, human erythrocytes were washed three times with PBS and were suspended in 150 mM NaCl–15 mM sodium citrate (pH 5.0) at a concentration of 7×10^7 cells per ml. Peptides were diluted in 150 mM NaCl–15 mM sodium citrate (pH 5.0) in a 96-well plate. Erythrocyte suspension (75 μl) was added to each well. The plate was incubated for 60 min at 37°C with shaking every 15 min. Unlysed erythrocytes were pelleted, and hemolysis was determined visually.

RESULTS

Purification of NSP4. The NSP4-containing cell lysate was loaded onto a QMA column and eluted at 0.7 M NaCl. Following the first elution, NSP4 was purified to about 30% purity. However, following a second elution off the QMA column, the NSP4 was at least 70% pure as shown by silver staining (Fig. 1A, lane 2) and Western blot analyses with an $NSP4_{114–135}$ peptide-specific antiserum (Fig. 1B, lane 3). In SA11-infected MA104 cells (Fig. 1B, lanes 2 and 3), the fully glycosylated NSP4 of apparent molecular weight of 28,000 (28K protein) is the major form of NSP4 detected, whereas very little of the 26K (single-site glycosylated) and 20K (nonglycosylated) forms of NSP4 are detected (26, 37). In contrast, in recombinant baculovirus-infected Sf9 cells, both the 28K and 26K forms of NSP4 are detected (Fig. 1). This phenomenon is thought to be due to the low temperature (27°C) used for Sf9 cell growth, which reduces the efficiency of glycosylation in insect cells. The migration of the fully glycosylated 28K NSP4 from insect cells is always slightly faster than that of the 28K NSP4 from MA104 cells when examined by SDS-PAGE (37). However, the migration of the 20K form of NSP4 in both systems is identical. The difference in migration of the 28K NSP4 is thought to result from differences in the glycosylation and trimming processes in the two systems. In addition, oligomeric forms of NSP4 ranging from 45K to 66K were observed in the purified NSP4 as detected by silver stain (Fig. 1A, lane 2) and confirmed by Western blotting (Fig. 1B, lane 3). These oligomers are thought to be a mixture of homodimers and heterodimers of the different forms of NSP4. In some experiments, NSP4 was further purified by immunoaffinity chromatography. This highly purified protein was at least 90% pure, and it had a similar profile to that shown in Fig. 1B when analyzed by Western blotting (data not shown).

MDA of NSP4 measured by liposome leakage assays. A liposome leakage assay was used to test whether NSP4 has MDA. In this system, MDA was monitored by the release of a fluorescent marker encapsulated into liposomes. When 10 μM

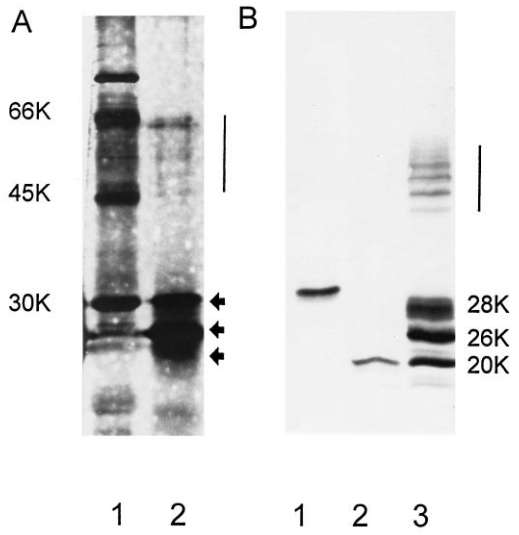

FIG. 1. Purification of NSP4. (A) Purity of NSP4 by silver stain. Lanes: 1, low-range molecular weight markers; 2, purified NSP4. The arrows show the three major bands (28K, 26K, and 20K) of NSP4. The vertical lines indicate oligomeric forms of NSP4. (B) Western blot. The 28K glycosylated NSP4 (lane 1) and 20K nonglycosylated NSP4 (lane 2) were from MA104 cells infected with SA11 rotavirus in the absence (lane 1) and the presence (lane 2) of tunicamycin. Lane 3 contains purified NSP4 from recombinant baculovirus-infected Sf9 cells. Three major bands (28K, 26K, and 20K) of NSP4 identified by silver staining were confirmed by Western blotting with an $NSP4_{114–135}$ peptide-specific antibody. The 28K, 26K, and 20K bands represent full-length NSP4 with two, one, and no sites glycosylated, respectively (26).

purified NSP4 was added to the liposomes, over 90% of the trapped dye was released from the liposomes (Fig. 2A). These data suggest that NSP4 has a direct effect on liposomes. A rotavirus structural protein, VP6, was used as a control in this study. VP6 tested at a final concentration of 12 μM did not have any MDA (Fig. 2B).

MDA of a synthetic peptide of $NSP4_{114–135}$. To determine if a specific domain in NSP4 is responsible for the MDA of NSP4, several synthetic peptides were tested for MDA. One of the peptides tested, $NSP4_{114–135}$, has a predicted amphipathic alpha-helical structure and is capable of mobilizing calcium release from the ER (36). Similar to the intact protein, when the $NSP4_{114–135}$ peptide was added to the liposomes, fluorescent dye was released (Fig. 3A). The amount of fluorescent dye released from the liposomes by the $NSP4_{114–135}$ peptide was dose dependent; 4 μM $NSP4_{114–135}$ released all the trapped dye in the liposomes in 10 min, and 2, 1, and 0.5 μM $NSP4_{114–135}$ released 82, 48, and 25% of the dye, respectively. Increasing the amount of the $NSP4_{114–135}$ peptide resulted in a faster release of the trapped dye, such that it was released in less than 1 min when the liposomes were incubated with the $NSP4_{114–135}$ peptide at 10 μM. Other synthetic peptides tested for MDA included synthetic peptides from amino acids (aa) 2 to 22 and aa 90 to 123 of NSP4 ($NSP4_{2–22}$ and $NSP4_{90–123}$, respectively), a Norwalk virus-specific peptide (NVSP), and a Norwalk virus C-terminal peptide (NVCP) which has a predicted amphipathic alpha-helical structure (17) similar to the $NSP4_{114–135}$ peptide. These peptides did not result in a significant release of fluorescent dye from liposomes, indicating the specificity of the $NSP4_{114–135}$ peptide MDA (Fig. 3B). These results suggest that the $NSP4_{114–135}$ peptide had a direct effect on liposomes and that release of the trapped dye did not require the presence of other viral or cellular factors.

Antibody-blocking assay. To further determine if aa 114 to 135 are involved in the MDA of NSP4, purified NSP4 was incubated with purified IgG from the $NSP4_{114–135}$ peptide antiserum and the mixture was analyzed in the liposome leakage assay. No protection was observed when the NSP4 protein was preincubated with preimmune IgG. However, preincubation of NSP4 with the anti-$NSP4_{114–135}$ peptide IgG significantly reduced the MDA of the protein (Fig. 4). These data confirm that at least part of the MDA of NSP4 localizes to the region between aa 114 and 135.

Effect of divalent ions and medium pH on the MDA of the $NSP4_{114–135}$ peptide. The presence of some divalent ions such as calcium, magnesium, or zinc protects cytoplasmic membranes (6). Ruiz et al. (30) reported that interactions between trypsinized rotavirus particles and isolated membrane vesicles from enterocytes are inhibited in the presence of 1 mM calcium. The ER has been recognized as an internal calcium store, with calcium levels estimated to be in the millimolar range (8), which is >10,000-fold higher than that in the cytoplasm (100 nM). Therefore, we tested if physiologic concentrations of calcium similar to the calcium concentration in the cytoplasm would increase the resistance of membranes to the MDA of the NSP4 protein and the $NSP4_{114–135}$ peptide (Fig. 5A). The cytoplasmic concentration of calcium tested (100 nM) had no effect on the MDA of purified NSP4 protein and the $NSP4_{114–135}$ peptide. The MDA of purified NSP4 protein was not inhibited and the MDA of the $NSP4_{114–135}$ peptide was slightly inhibited at a calcium concentration higher than at a normal intracellular calcium concentration (100 nM). The MDA of the $NSP4_{114–135}$ peptide (2 μM) was lower in the presence of 10 mM Ca^{2+} (80%) than in the absence of Ca^{2+} (100%) or in the presence of 100 nM Ca^{2+} (98%).

Many lytic peptides have MDA only at an acidic pH (15, 25, 32, 38). We further tested the MDA of $NSP4_{114–135}$ peptide at the different pHs to determine if it mimics the properties of other known lytic peptides. The purified NSP4 and the $NSP4_{114–135}$ peptide showed MDA at both a normal cellular physiologic pH and an acidic pH (Fig. 5B). Thus, the $NSP4_{114–135}$ peptide functions over a broader pH range than do other lytic peptides. Likewise, the $NSP4_{114–135}$ peptide sequence does not correspond to that of any of the previously classified lytic peptides (33).

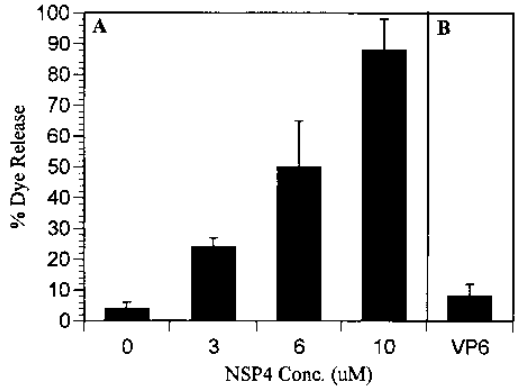

FIG. 2. Dose-dependent effect of NSP4 on liposomes. (A) Various concentrations (0 to 10 μM) of NSP4 (shown on the *x* axis) were incubated with liposomes at room temperature for 10 min in sodium citrate buffer (pH 6.0). The amount of fluorescent dye released from the liposomes immediately after this 10-min incubation was calculated relative to the percentage of total dye released after treatment with Triton X-100 and plotted on the *y* axis (mean and standard deviation; $n = 3$). PBS (NSP4 concentration, 0 μM) was used to determine background leakage. (B) A rotavirus structural protein, VP6 (12 μM), was used as a control.

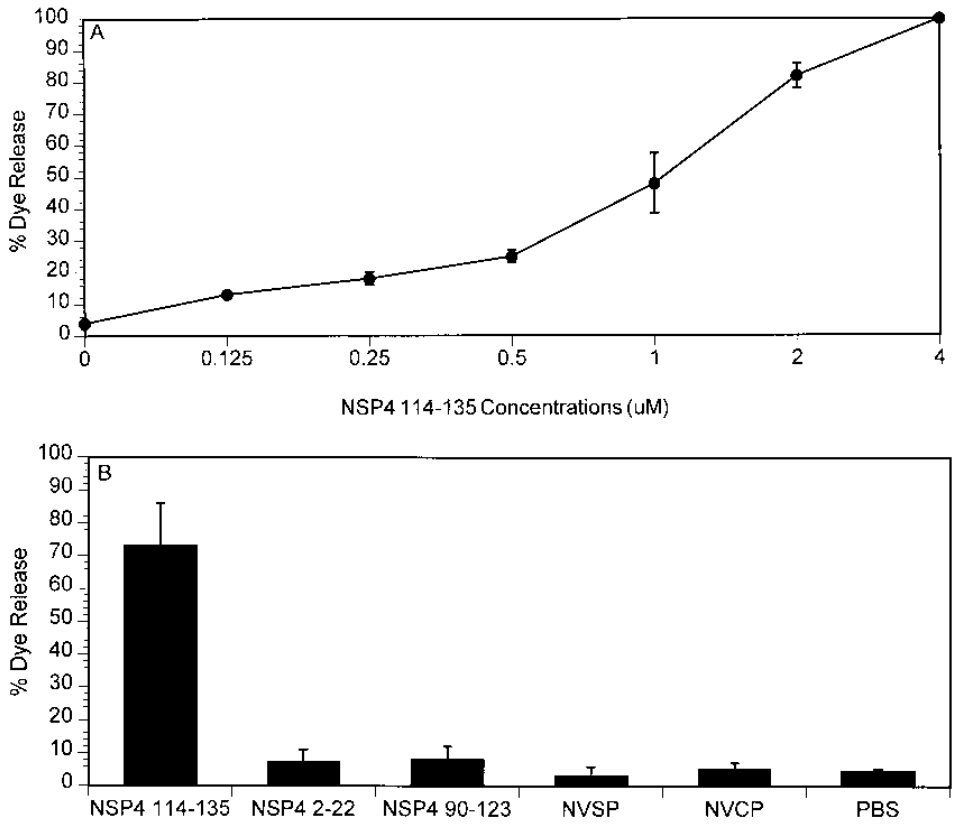

FIG. 3. (A) Dose-dependent effect of the $NSP4_{114–135}$ peptide on liposomes. The $NSP4_{114–135}$ peptide caused release of fluorescent dye from PC liposomes at various concentrations (0 to 4 μM). PBS (NSP4 concentration, 0 μM) was used to determine background leakage. The concentrations of the $NSP4_{114–135}$ peptide are shown on the *x* axis, and the percentage of dye release is shown on the *y* axis (mean ± standard deviation; $n = 3$). (B) The specificity of dye release induced by the $NSP4_{114–135}$ peptide. The $NSP4_{114–135}$, $NSP4_{2–22}$, $NSP4_{90–123}$, NVSP, and NVCP peptides (shown on the *x* axis) were individually incubated at 2 μM with liposomes for 5 min at room temperature in sodium citrate buffer (pH 6.0). The amount of fluorescent dye released from liposomes immediately after this 5-min incubation was calculated relative to the percentage of total dye released after treatment with Triton X-100 (shown on the *y* axis). Only the $NSP4_{114–135}$ peptide showed a significant increase in release of fluorescent dye.

Liposomes and microsomes are damaged by NSP4 and $NSP4_{114–135}$. Taken together, the previous results show that NSP4 and the $NSP4_{114–135}$ peptide directly release fluorescent dye from liposomes. However, it remained unclear if NSP4 or the $NSP4_{114–135}$ peptide release dye from the liposomes by disrupting the membranes or by functioning as a specific channel or pore in liposomes. To evaluate this question, liposomes, microsomes (ER), and Sendai virus (representing cytoplasmic

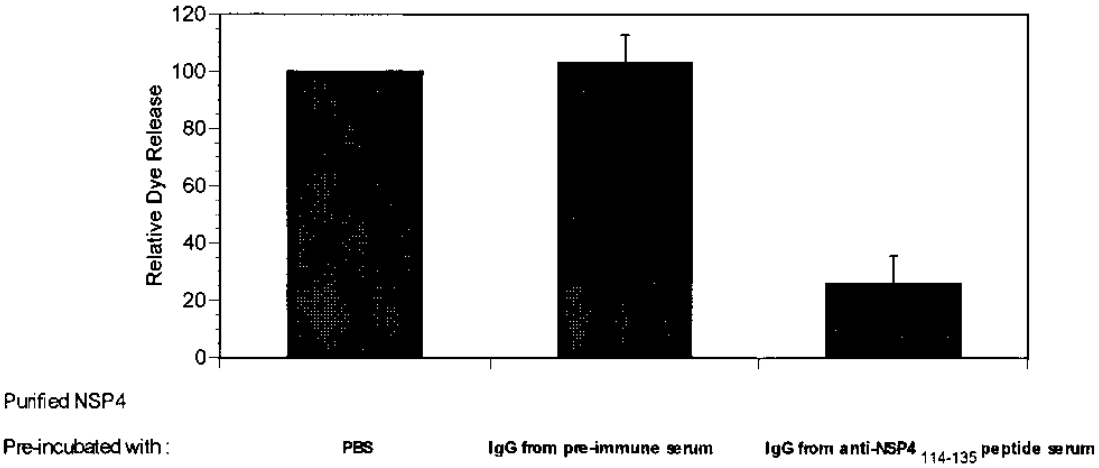

FIG. 4. Antibody-blocking assay. Highly purified NSP4 (10 μM) was incubated with purified $NSP4_{114–135}$ peptide-specific IgG and then with liposomes. The amount of fluorescent dye released from liposomes incubated with purified NSP4 pretreated with preimmune IgG or pretreated with $NSP4_{114–135}$ peptide-specific IgG was calculated relative to the percentage of total dye released from liposomes incubated with purified NSP4 pretreated with PBS (mean ± standard deviation; $n = 3$ [shown on the *y* axis]).

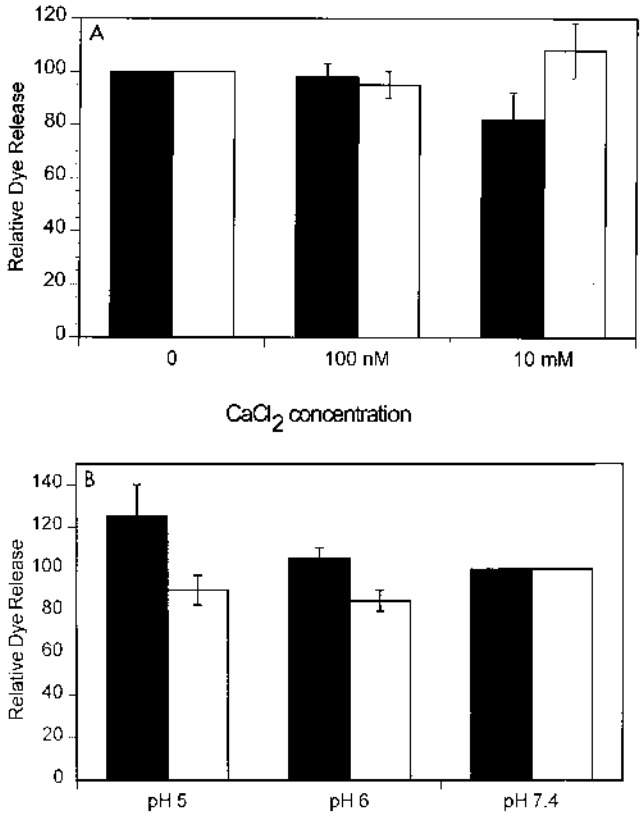

FIG. 5. (A) The $NSP4_{114–135}$ peptide releases fluorescent dye from PC liposomes in the presence or absence of calcium. Liposomes were incubated for 10 min with highly purified NSP4 (10 μM) (□) or the $NSP4_{114–135}$ peptide (2 μM) (■) in the presence of 0, 100 nM, or 10 mM $CaCl_2$ (shown on the *x* axis). The amount of fluorescent dye released from liposomes incubated in the presence of calcium was calculated relative to the percentage of total dye released from liposomes in the absence of calcium (mean ± standard deviation; $n = 3$ [shown on the *y* axis]). (B) The effect of pH on dye release induced by highly purified NSP4 (10 μM) (□) or $NSP4_{114–135}$ peptide (2 μM) (■). The amount of fluorescent dye released from liposomes incubated at lower pH (pH 5 and pH 6) was calculated relative to the percentage of total dye released from liposomes incubated at physiologic pH (pH 7.4, mean ± standard deviation; $n = 3$ [shown on the *y* axis]).

membranes) were each incubated with NSP4 protein or the $NSP4_{114–135}$ peptide (Fig. 6). Similar results were observed with purified NSP4 protein at 6 μM for liposomes and 12 μM for microsomes (data not shown) when compared with the $NSP4_{114–135}$ peptide at 40 μM for liposomes and 200 μM for microsomes. The liposomes were heterogeneous, ranging from 25 to 100 nm in diameter (Fig. 6A). The liposomes were incubated with PBS (Fig. 6A), control NVCP peptide (Fig. 6B), $NSP4_{114–135}$ peptide (Fig. 6C), or $NSP4_{90–123}$ peptide (data not shown) and observed for broken liposomes. Disruptions were observed only with the liposomes treated with the $NSP4_{114–135}$ peptide or NSP4 (data not shown). The large liposomes (100 nm in diameter, containing multiple layers) were resistant to the $NSP4_{114–135}$ peptide and SDS (data not shown). The disruption was specific, because broken microsomes were observed when the microsomes were incubated with $NSP4_{114–135}$ (Fig. 6F) but not with PBS (Fig. 6D) or NVCP (Fig. 6E). To determine if the MDA of the $NSP4_{114–135}$ peptide was specific to the ER membrane, Sendai virus, whose envelope is composed of cytoplasmic membranes, was incubated with $NSP4_{114–135}$ (200 μM) or JTS-1 (20 μM), a known lytic peptide (15). Broken enveloped viruses were observed when Sendai virus was incubated with JTS-1 (Fig. 6H) but not when it was incubated with the $NSP4_{114–135}$ peptide (Fig. 6I), indicating that the MDA of the $NSP4_{114–135}$ peptide was not functional with cytoplasmic membranes.

NSP4 protein and the $NSP4_{114–135}$ peptide have no MDA on cytoplasmic membranes. It is possible that the Sendai virion is not completely representative of cytoplasmic membranes. Therefore, we tested if the cytoplasmic membrane is damaged by NSP4 protein or the $NSP4_{114–135}$ peptide in two other systems. Human erythrocytes were incubated with the $NSP4_{114–135}$ peptide (200 μM) or the amphipathic membrane-active peptide, JTS-1 (2 μM), and hemolysis was monitored. Notably, hemolysis was observed only in JTS-1-treated cells.

To further investigate if the NSP4 protein and the $NSP4_{114–135}$ peptide had any MDA on cytoplasmic membranes, NSP4 protein, the $NSP4_{114–135}$ peptide, or JTS-1 was added to Sf9 cells loaded with fura-2. The membrane activity of the amphipathic membrane-active peptide (JTS-1) was shown in vitro by performing liposome leakage assays and in vivo by measuring reporter gene activity delivered by JTS-1–DNA complexes (15). When JTS-1 (2 μM) was added to Sf9 cells (pH 6), the cytoplasmic membrane was damaged, as indicated by a continual increase in $[Ca^{2+}]_i$ levels due to the influx of extracellular calcium (Fig. 7, trace c). The addition of Triton X-100 to cells exposed to JTS-1 peptide had little effect on further increasing the $[Ca^{2+}]_i$ levels (data not shown because it was out of the range of the *y* axis). These results suggest that the cytoplasmic membrane was damaged by the addition of the JTS-1 peptide to cells.

In contrast, the addition of 6 μM NSP4 protein (Fig. 7, trace a) or 100 μM the $NSP4_{114–135}$ peptide (trace b) to cells resulted in only a small increase in $[Ca^{2+}]_i$ levels. The elevation in $[Ca^{2+}]_i$ levels caused by NSP4 protein was transient, and the concentration returned to the normal range in a short time (2 min). The changes in the intracellular calcium concentration that were induced by the $NSP4_{114–135}$ peptide were smaller and were sustained for a longer period (at least 4 min) than were those seen with the NSP4 protein. These results indicate that the cytoplasmic membrane remained intact and the regulatory mechanisms in the cytoplasmic membranes, such as the ATPase pump, remained functionally normal. More importantly, NSP4 and the $NSP4_{114–135}$ peptide cause an increase in intracellular calcium levels in the absence of extracellular calcium (36). These results suggest that the increase in calcium concentration observed in Sf9 cells as a result of NSP4 and the $NSP4_{114–135}$ peptide is not caused by cytoplasmic membrane disruption. As we have shown previously, the increase induced by exogenously added NSP4 protein or peptide is mediated by a PLC-stimulated pathway which probably functions by opening the calcium channels on the ER membrane (36). Taken together, these results indicate that the ER membrane is more sensitive to the MDA of NSP4 than is the cytoplasmic membrane.

DISCUSSION

We previously reported that the expression of NSP4 in Sf9 cells causes a significant increase in $[Ca^{2+}]_i$ (37). Recently, we showed that increases in $[Ca^{2+}]_i$ seen in insect cells expressing NSP4 result from mobilization of calcium from the ER (36). Calcium release from the ER is also observed when purified NSP4 or the $NSP4_{114–135}$ peptide is added exogenously to uninfected insect cells (36). U-73122, a PLC inhibitor, blocks the calcium release if added before the administration of NSP4 or $NSP4_{114–135}$ peptide to uninfected insect cells (36). However, the addition of the PLC inhibitor to cells expressing NSP4

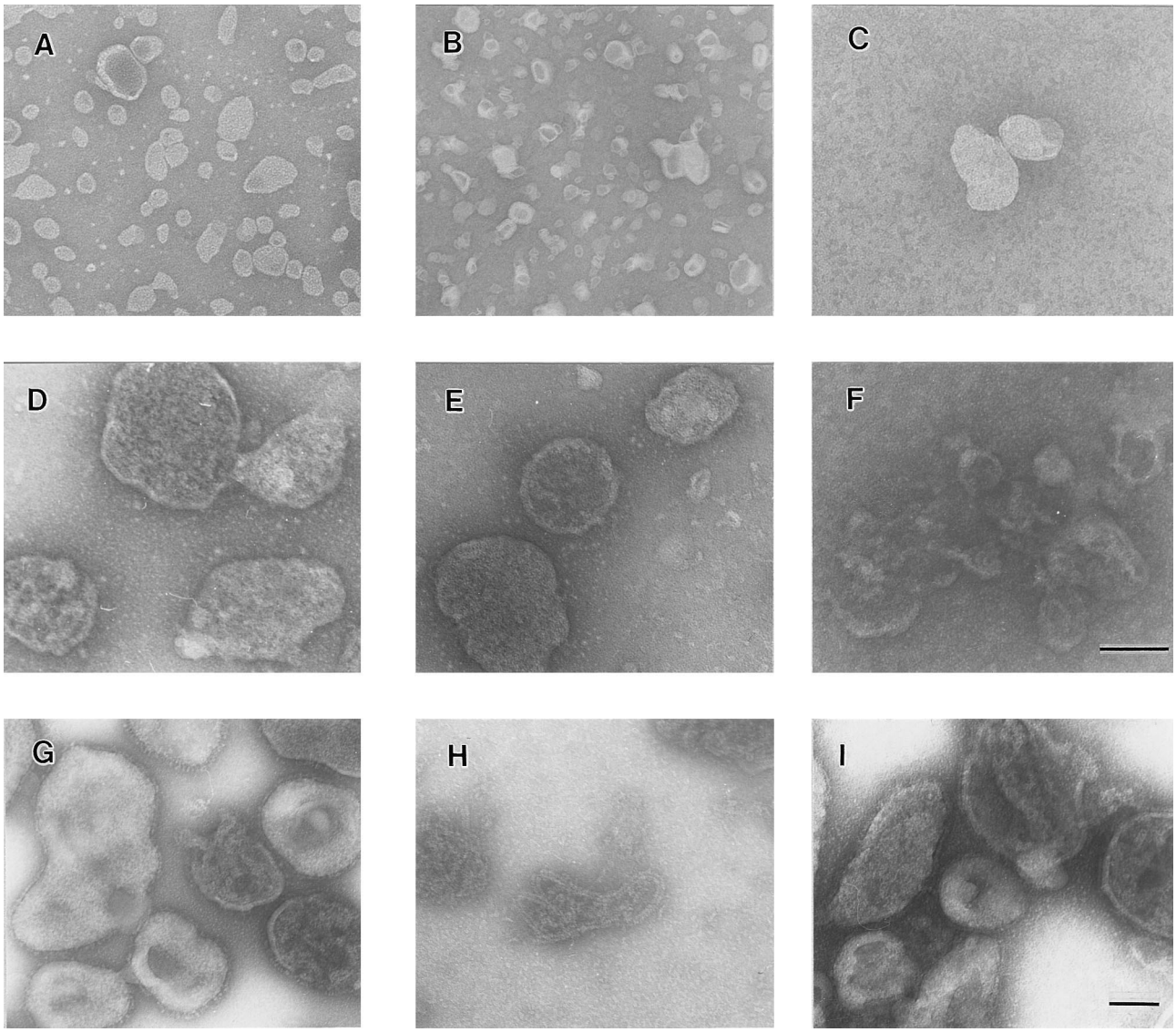

FIG. 6. Visualization of liposomes and microsomes incubated in the presence or absence of the synthetic peptides. Liposomes (2 μl) were incubated for 10 min with PBS (A), 40 μM NVCP (B), and 40 μM $NSP4_{114–135}$ (C). Microsomes (1 μl) were incubated for 10 min with PBS (D), 200 μM NVCP (E), and 200 μM $NSP4_{114–135}$ (F). Sendai virus (1 μl) was incubated for 10 min with PBS (G), 20 μM JTS-1 (H), or 200 μM $NSP4_{114–135}$ (I). Samples were stained with 1% ammonium molybdate and observed by EM. Panels A through F are the same magnification, and the bar shown in panel F represents 100 nm. Panels G through I are the same magnification, and the bar in panel I represents 100 nm.

endogenously does not lower the increased $[Ca^{2+}]_i$ levels. In addition, the exogenous administration of the $NSP4_{114–135}$ peptide to cells endogenously expressing NSP4 further elevates $[Ca^{2+}]_i$ levels. The basal calcium permeability of the ER in insect cells endogenously expressing NSP4 was evaluated by measuring the release of calcium induced by ionomycin (a calcium ionophore) or thapsigargin (an inhibitor of the ER Ca^{2+}-ATPase pump) (35). These results suggest that two distinct pathways are responsible for the increased $[Ca^{2+}]_i$ in insect cells. We have hypothesized that the NSP4 protein, or putative cleavage products containing the C terminus of NSP4, released from cells might bind to a cellular receptor, stimulating the PLC-$InsP_3$ pathway (36). We now propose that the endogenously expressed NSP4 might have a direct effect on the ER membrane and cause permeability changes.

To test our hypothesis, we first purified NSP4 from recombinant baculovirus-infected Sf9 cells. NSP4 is a nonstructural ER transmembrane glycoprotein encoded by gene 10 of group A rotavirus. NSP4 has two N-linked oligosaccharide sites at the N terminus which is on the luminal side of the ER. The transmembrane and membrane association properties of NSP4 make purification of NSP4 difficult. However, after ion-exchange FPLC, NSP4 was enriched to at least 70% purity. Multiple forms of NSP4 based on different glycosylation patterns, including the 28K, 26K, and 20K forms and oligomers of NSP4, were purified by this procedure. Further purification of NSP4 was achieved by immunoaffinity chromatography.

Liposomes have been used as a model to understand the fusion, lytic, and membrane destabilization activity of many proteins and peptides (7, 12, 15, 22, 23, 25, 29, 38). These membrane activities are monitored by the release of a fluorescent marker encapsulated into liposomes. The purified NSP4

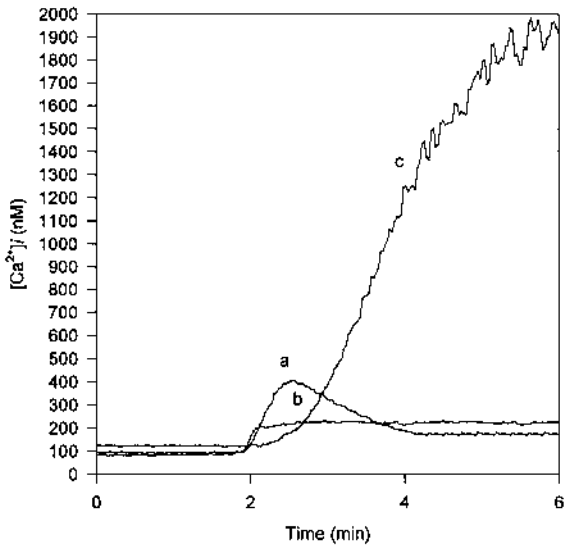

FIG. 7. Graphical depiction of the $[Ca^{2+}]_i$ changes induced by NSP4 (trace a), the $NSP4_{114–135}$ peptide (trace b), or JTS-1 peptide (trace c). NSP4 (6 μM), $NSP4_{114–135}$ (100 μM), or JTS-1 (2 μM) was added to fura-2-loaded Sf9 cells. $[Ca^{2+}]_i$ levels were measured before and after addition of the protein or peptides.

showed MDA by the liposome leakage assay. To determine the specificity of the MDA induced by the purified NSP4 and to further determine the active domain of NSP4 responsible for the MDA, we tested the MDA of several synthetic peptides. The $NSP4_{114–135}$ peptide, but not other peptides including $NSP4_{2–22}$, $NSP4_{90–123}$, and NVCP or the protein VP6, possessed MDA. The specificity of the MDA of NSP4 was further confirmed by antibody-blocking assays. In addition, when the active peptide was iodinated with unlabeled iodine or tyrosine 131 in the peptide was replaced by lysine, the MDA of the altered $NSP4_{114–135}$ peptide was reduced or completely abolished (data not shown). These results suggest that aa 114 to 135 is at least part of the functional domain of the NSP4 protein and that tyrosine 131 appears to be important for the function and possibly the structure of NSP4. Further studies are needed to determine if tyrosine 131 by itself, or a conformational change, results in the abolition of the MDA of NSP4.

Data from other investigators indicate that the functional properties of amphipathic alpha-helixes may include lipid association, membrane perturbation in the forms of fusion or lysis, hormone receptor catalysis, and transmembrane signal transduction (33). Amphipathic helical domains have been described in some lipid-associated proteins including endorphins, polypeptide venoms such as bombolitin and melittin, polypeptide antibiotics such as magainin, and certain complex transmembrane proteins such as bacteriorhodopsin (33). Membrane destabilization activity has been found in native proteins or peptides such as melittin (10), the synthetic amphipathic peptide GALA (25), and viral envelope proteins such as the 26-aa N-terminal peptide from the G-protein of vesicular stomatitis virus (31, 32), the N-terminal peptide of Sendai virus F protein, the 20-aa peptide (HA peptide) of influenza virus (22, 29), the cytolytic peptide of lentivirus TM protein (20, 21), and a pH-dependent membrane-active peptide, JTS-1 (15). In contrast to these lytic peptides, $NSP4_{114–135}$ peptide has a specific effect on ER membranes but not on cytoplasmic membranes. This is the first report to our knowledge describing a viral protein or peptide which has MDA specific to the ER membrane.

In liposome leakage assays, a smaller amount of $NSP4_{114–135}$ peptide (4 μM) than of purified NSP4 protein (10 μM) causes dye release. This may be due to a lower solubility in sodium citrate buffer of the NSP4 protein than of the $NSP4_{114–135}$ peptide. Clearly, the effect of the MDA of NSP4 protein in PBS (10 μM) was greater than that of the $NSP4_{114–135}$ peptide in PBS (40 μM) by EM observations. Several possible reasons explain these differences: (i) the peptide does not present the entire functional domain, (ii) the peptide does not adopt the correct native conformation, (iii) other domains in NSP4 in addition to aa 114 to 135 play a role in MDA, and (iv) the glycosylation of NSP4 might enhance the MDA activity of NSP4. It is unlikely that tiny amounts of cellular proteins in the partially purified NSP4 enhance the MDA of NSP4. Recently, we have further purified the NSP4 protein by immunoaffinity column chromatography (data not shown). The MDA in the liposome leakage assays of this highly purified NSP4 (>90% pure) is the same as that of the semipurified protein tested in the studies described in this paper.

The liposome leakage assay and visualization of the ER membrane damage following the addition of NSP4 or the $NSP4_{114–135}$ peptide provided direct evidence of ER membrane disruption by NSP4. NSP4 protein at 6 μM and the $NSP4_{114–135}$ peptide at 40 μM caused liposome damage. Higher concentrations of NSP4 (12 μM) and the $NSP4_{114–135}$ peptide (200 μM) were required for the microsome membrane damage (observed by EM) than the concentrations used in the liposome leakage assays. This might be due to the difference in the sensitivities of the assays. In addition, the presence of a larger amount of cholesterol in the ER membranes enhances the flexibility and stability of the membrane (1).

Interactions of trypsinized rotavirus particles with liposomes (23) and isolated cytoplasmic membrane vesicles from enterocytes (30) have been reported. Trypsinized triple-layered rotavirus particles release fluorescent dye trapped in liposomes and in isolated cytoplasmic membrane vesicles from enterocytes. However, rotavirus particles with uncleaved VP4 do not interact with membranes. Recently, Falconer et al. (14) reported that trypsin activation is necessary for rotavirus to mediate cell-cell fusion. These results suggest that rotavirus virions enter cells through direct penetration of the plasma membrane mediated by cleaved triple-layered particles by an unknown mechanism. However, VP4 is not likely to be cleaved in the cytoplasm of cells, because the VP4 remains uncleaved in newly made triple-layered particles. Therefore, it is unlikely that newly made triple-layered particles have an effect on ER membranes in the cytoplasm.

The specific disruption of ER membranes by NSP4 described in this report is consistent with our previous observations. Our previous work suggested that endogenously expressed NSP4 in insect cells increases the basal calcium permeability of ER membranes but not cytoplasmic membranes by a mechanism other than the PLC-mediated pathway (36). More importantly, the MDA of NSP4 could explain how the transient envelope is removed during rotaviral morphogenesis. However, details of when and how the envelope is removed remain unclear. If the MDA of NSP4 is activated as soon as NSP4 is expressed and expression continues throughout the virus replication cycle, this activity could disrupt the ER membranes, resulting in cell death even before progeny viral particles are made. We propose that interactions between NSP4 and other rotavirus proteins affect the MDA of NSP4. This hypothesis is based on the following observations: (i) Poruchynsky et al. (28) reported that NSP4 forms heterooligomers with VP4; (ii) Au et al. (3) reported that a VP4-binding site is located between aa 112 and 146 of NSP4; (iii) we have

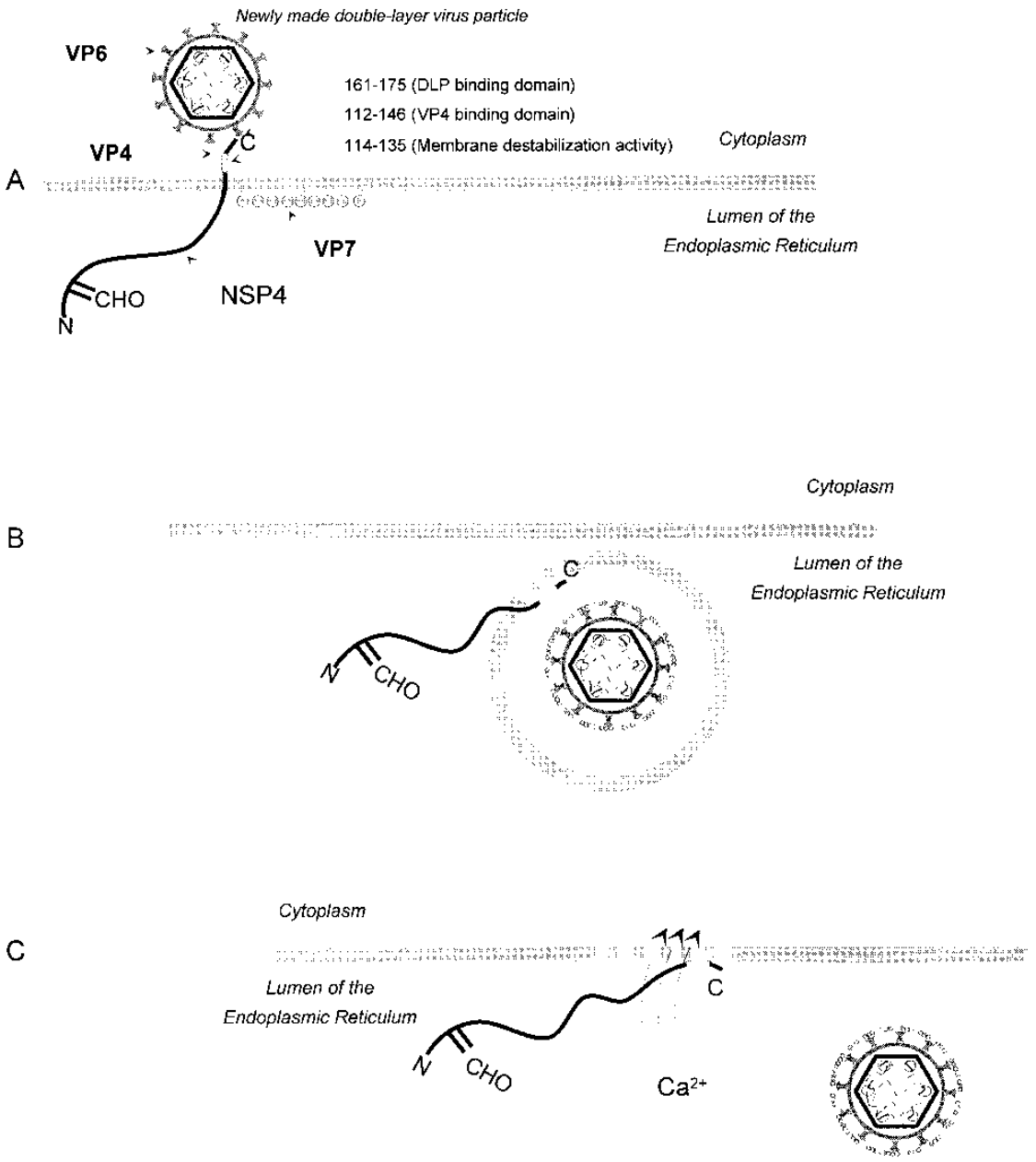

FIG. 8. Proposed model for removal of the transient envelope by NSP4 during rotavirus morphogenesis. (A) The newly synthesized double-layered particles (DLP) in the cytoplasm bind the C terminus of NSP4 and bud into the lumen of the ER. VP4 binds NSP4 and occupies the MDA site. (B) VP7 undergoes a rearrangement and relocates to the interior of the enveloped particle during the budding process (27). VP7 interacts with VP4 inside the enveloped particles and forms the outer shell of the triple-layered particles. This releases the MDA of NSP4 and exposes the MDA domain. (C) The MDA of NSP4 removes the envelope, possibly by changing the permeability of the ER. and ● represent VP4 and VP7, respectively. CHO represents glycosylation sites on NSP4. N and C represents the N terminus and C terminus, respectively, of NSP4. ▭ represents the MDA domain of NSP4.

shown that the NSP4 MDA is inclusive of residues 114 to 135, which overlaps with part of the putative VP4-binding domain; and (iv) VP4 and VP7 form the outer shell of the mature viral particles, which do not contain NSP4.

We hypothesize that the interactions between NSP4, VP4, and VP7 play an important role in regulating the MDA of NSP4, and we propose a model for rotavirus morphogenesis (Fig. 8). One possibility is that after the synthesis of NSP4, the C terminus of NSP4 in the cytoplasm is bound to VP4. This interaction between NSP4 and VP4 could block the MDA by directly occupying the MDA domain or by changing the conformation of the MDA domain in NSP4. It has been proposed that when viral particles bud into the ER, VP7 repositions itself from its location in the lumen of the ER to the interior of the enveloped viral particles (27). When VP7 and VP4 assemble into the outer shell of the virus, VP4 would no longer associate with NSP4. Therefore, the MDA of NSP4 would be exposed and activated. This activation of the MDA of NSP4

could result in the removal of the transient envelope. This model provides a mechanism of how the transient membrane of subviral particles is removed in the ER prior to release from the cell, which will need to be tested by further experiments.

ACKNOWLEDGMENTS

This work was supported by Public Health Service grant DK 30144 from the National Institute of Diabetes and Digestive and Kidney Diseases.

We thank Stephen Gottschalk, Department of Cell Biology, Baylor College of Medicine, for assistance in the initial preparation of the liposomes. We also thank Stephen Gottschalk and Louis Smith, Department of Medicine, Baylor College of Medicine, for providing the amphipathic membrane-active peptide JTS-1. We thank Christopher Barone for help with the illustration of our model, Ronald E. Montelaro for helpful discussions, and Kazi Islam for purification of the synthetic peptides.

REFERENCES

1. **Alberts, B., D. Bray, J. Lewis, M. Raff, K. Roberts, and J. D. Watson.** 1989. Molecular biology of the cell, p. 279–283. Garland Publishing, Inc., New York.
2. **Au, K. S., W. K. Chan, J. W. Burns, and M. K. Estes.** 1989. Receptor activity of rotavirus nonstructural glycoprotein NS28. J. Virol. **63:**4553–4562.
3. **Au, K.-S., N. M. Mattion, and M. K. Estes.** 1993. A subviral particle binding domain on the rotavirus nonstructural glycoprotein NS28. Virology **194:**665–673.
4. **Ball, J. M., N. L. Henry, R. C. Montelaro, and M. J. Newman.** 1994. A versatile synthetic peptide-based ELISA for identifying antibody epitopes. J. Immunol. Methods **171:**37–44.
5. **Ball, J. M., P. Tian, C. Q.-Y. Zeng, A. Morris, and M. K. Estes.** 1996. Age-dependent diarrhea is induced by a viral nonstructural glycoprotein. Science **272:**101–104.
6. **Bashford, C. L., G. M. Alder, M. Gianfranco, K. J. Micklem, J. J. Murphy, and C. A. Pasternak.** 1986. Membrane damage by hemolytic viruses, toxins, complement, and other cytotoxic agents. J. Biol. Chem. **261:**9300–9308.
7. **Blumenthal, R.** 1986. pH-dependent lysis of liposomes by adenovirus. Biochemistry **25:**2231–2237.
8. **Carafoli, E.** 1987. Intracellular calcium homeostasis. Annu. Rev. Biochem. **56:**395–433.
9. **Carpino, L. A., and G. Y. Han.** 1972. 9-Fluorenylmethoxycarboyl amino-protecting group. J. Org. Chem. **37:**3404–3409.
10. **Dempsey, C. E.** 1990. The actions of melittin on membranes. Biochim. Biophys. Acta **1031:**143–161.
11. **Dubois-Dalcq, M., K. V. Holmes, and B. Rentier.** 1984. Assembly of enveloped RNA viruses. Springer-Verlag, Inc., New York.
12. **Duzgunes, N., and S. A. Shavnin.** 1992. Membrane destabilization by N-terminal peptides of viral envelope proteins. J. Membr. Biol. **128:**71–80.
13. **Estes, M. K., and J. Cohen.** 1989. Rotavirus gene structure and function. Microbiol. Rev. **53:**410–449.
14. **Falconer, M. M., J. M. Gilbert, A. M. Roper, H. B. Greenberg, and J. S. Gavora.** 1995. Rotavirus-induced fusion from without in tissue culture cells. J. Virol. **69:**5582–5591.
15. **Gottschalk, S., J. T. Sparrow, F. E. Leland, M. P. Mims, S. L. C. Woo, and L. C. Smith.** 1995. A novel DNA/peptide complex for efficient gene transfer and expression in mammalian cells. Gene Ther. **3:**448–457.
16. **Grynkiewicz, G., P. Martin, and R. Y. Tsien.** 1985. A new generation of Ca^{2+} indicators with greatly improved fluorescence properties. J. Biol. Chem. **260:**3440–3450.
17. **Margolikf, H., J. L. Spouge, J. L. Cornette, K. B. Cease, C. Delisi, and J. A. Berzofsky.** 1987. Prediction of immunodominant helper T cell antigenic sites from the primary sequence. J. Immunol. **138:**2213–2229.
18. **McKinney, M. M., and A. Parkinson.** 1987. A simple, non-chromatographic procedure to purify immunoglobulins from serum and ascites fluid. J. Immunol. Methods **96:**271–278.
19. **Meyer, J. C., C. C. Bergmann, and A. R. Bellamy.** 1989. Interaction of rotavirus cores with the nonstructural glycoprotein NS28. Virology **171:**98–107.
20. **Miller, M. A., M. W. Cloyd, J. Liebmann, C. R. Rinaldo, K. R. Islam, S. Z. S. Wang, T. A. Mietzner, and R. C. Montelaro.** 1993. Alterations in cell membrane permeability by the lentivirus lytic peptide (LLP-1) of HIV-1 transmembrane protein. Virology **196:**89–100.
21. **Miller, M. A., R. F. Garry, J. M. Jaynes, and R. C. Montelaro.** 1991. A structural correlation between lentivirus transmembrane proteins and natural cytolytic peptides. AIDS Res. Hum. Retroviruses **7:**511.
22. **Murata, M., S. Kagiwada, R. Hishida, R. Ishiguro, S. Ohnishi, and S. Takahashi.** 1991. Modification of the N-terminus of membrane fusion-active peptides blocks the fusion activity. Biochem. Biophys. Res. Commun. **179:** 1050–1055.
23. **Nandi, P., A. Charpilienne, and J. Cohen.** 1992. Interaction of rotavirus particles with liposomes. J. Virol. **66:**3363–3367.
24. **New, P. R. C.** 1990. Liposomes: a practical approach, p. 128–136. IRL Press, Oxford.
25. **Parente, R. A., S. Nir, and F. C. Szoka.** 1990. Mechanism of leakage of phospholipid vesicle contents induced by the peptide GALA. Biochemistry **29:**8720–8728.
26. **Petrie, B. L., M. K. Estes, and D. Y. Graham.** 1983. Effects of tunicamycin on rotavirus morphogenesis and infectivity. J. Virol. **46:**270–274.
27. **Poruchynsky, M. S., and P. H. Atkinson.** 1991. Rotavirus protein rearrangements in purified membrane-enveloped intermediate particles. J. Virol. **65:** 4720–4727.
28. **Poruchynsky, M. S., D. R. Maass, and P. H. Atkinson.** 1991. Calcium depletion blocks the maturation of rotavirus by altering the oligomerization of virus-encoded proteins in the ER. J. Cell Biol. **114:**651–661.
29. **Rafalski, M., A. Ortiz, A. Rockwell, L. C. van Ginkel, J. D. Lear, W. F. DeGrado, and J. Wilschut.** 1991. Membrane fusion activity of the influenza virus hemagglutinin: interaction of HA2 N-terminal peptides with phospholipid vesicles. Biochemistry **30:**10211–10220.
30. **Ruiz, M., S. R. Alonso-Torre, A. Charpilienne, M. Vasseur, F. Michelangeli, J. Cohen, and F. Alvarado.** 1994. Rotavirus interaction with isolated membrane vesicles. J. Virol. **68:**4009–4016.
31. **Schlegel, R., and M. Wade.** 1984. A synthetic peptide corresponding to the NH_2 terminus of vesicular stomatitis virus glycoprotein is a pH dependent hemolysin. J. Biol. Chem. **259:**4691–4694.
32. **Schlegel, R., and M. Wade.** 1985. Biologically active peptides of the vesicular stomatitis virus glycoprotein. J. Virol. **53:**319–323.
33. **Segrest, J. P., H. De Loof, J. G. Dohlman, C. G. Brouillette, and G. M. Anatharamaiah.** 1990. Amphipathic helix motif: classes and properties. Proteins Struct. Funct. Genet. **8:**103–117.
34. **Shuttleworth, T. J., and J. L. Thompson.** 1991. Effect of temperature on receptor-activated changes in $[Ca^{2+}]_i$ and their determination using fluorescent probes. J. Biol. Chem. **266:**1410–1414.
35. **Thastrup, O.** 1990. Role of Ca^{2+}-ATPases in regulation of cellular Ca2+ signalling, as studied with the selective microsomal Ca2(+)-ATPase inhibitor, thapsigargin. Agents Actions **29:**8–15.
36. **Tian, P., M. K. Estes, Y. Hu, J. M. Ball, C. Q.-Y. Zeng, and W. P. Schilling.** 1995. The rotavirus nonstructural glycoprotein NSP4 mobilizes Ca^{2+} from the endoplasmic reticulum. J. Virol. **69:**5763–5772.
37. **Tian, P., Y. Hu, W. P. Schilling, D. A. Lindsay, J. Eiden, and M. K. Estes.** 1994. The nonstructural glycoprotein of rotavirus affects intracellular calcium levels. J. Virol. **68:**251–257.
38. **Todt, J. C., W. J. Rocque, and E. J. McGroarty.** 1992. Effects of pH on bacterial porin function. Biochemistry **31:**10471–10478.
39. **Zeng, C. Q.-Y., M. J. Wentz, J. Cohen, M. K. Estes, and R. F. Ramig.** 1996. Characterization and replicase activity of double-layered and single-layered rotavirus-like particles expressed from baculovirus recombinants. J. Virol. **70:**2736–2742.
40. **Zeng, Q., M. Labbe, J. Cohen, B. V. V. Prasad, D. Chen, R. F. Ramig, and M. K. Estes.** 1994. Characterization of rotavirus VP2 particles. Virology **201:**55–65.